STUDIES CONCERNING CHARGED NICKEL HYDROXIDE ELECTRODES

PART V. VOLTAMMETRIC BEHAVIOUR OF ELECTRODES CONTAINING β-$Ni(OH)_2$

R. BARNARD and C. F. RANDELL

Berec Group Limited, Group Technical Centre, St. Ann's Road, London N15 3TJ (U.K.)

Summary

The first oxidation wave for aged β-$Ni(OH)_2$ normally occurs simultaneously with oxygen evolution, and by measuring the oxygen evolved the active material oxidation current may be determined. Oxidation of aged, β-$Ni(OH)_2$ (phase U) to β-NiOOH (phase V) reaches a maximum at about 0.59 V with respect to Hg/HgO/7M KOH whilst further oxidation to the γ-phase (V_1) takes place at higher potentials (0.66 V).

By restricting the anodic limit (0.55 - 0.6 V) the system can be constrained largely within the β-phase. At low oxidation states (2.1 - 2.2) a single reduction peak appears at ~ 0.4 V due to the reduction of phase V to phase U. If the oxidation state is increased to 2.7 by repetitive cycling or by single potentiostatic steps the reduction peak appears at progressively less cathodic potentials in the range 0.35 - 0.3 V. Cyclic oxidation reduction is found to "activate" the β-$Ni(OH)_2$ starting material allowing reoxidation to occur at lower anodic potentials (~ 0.46 V).

Shifts in cathodic potential are found to relate directly to a decrease in quasi-reversible potential by ~ 70 mV for the species present at the peak maxima. The broad reduction envelopes are considered to be related to differences in free energy between different pairs of coexisting phases, U and V, which are present within the β-phase layer lattice system. The previous charging history critically influences the extent to which the quasi-reversible potential (E_r) value changes. Additional kinetic factors also appear to influence the precise shape and position of the first oxidation wave for β-$Ni(OH)_2$ which has been aged in hot 7M KOH.

1. Introduction

Nickel hydroxide/oxyhydroxide layers have been studied extensively using cyclic voltammetry. Comparatively few studies have been reported for sintered plate electrodes, however, and the cause of hysteresis on charge/discharge cycling has not been satisfactorily explained [1].

0378-7753/83/0000-0000/$3.00

Until recently [2 - 4] the potentials of the two β-phase (U/V) and α/γ-phase (U_1/V_1) couples and their alkali and water dependences had not been clearly established. Both the α- and β-$Ni(OH)_2$ layer-lattices have various degrees of disorder giving rise to couples having different standard potentials. This effect may also be responsible for some hysteresis [5]. Several oxidation/reduction peaks could therefore be expected in the cyclic voltammograms.

MacArthur [6] demonstrated, in keeping with the earlier observations by Bode *et al.* [7, 8], that it is possible to cycle between α/γ-phase structures for a limited time. It was also clearly demonstrated that, after ageing, oxidation of the hydroxide shifted to more anodic potentials. This transformation was ascribed to oxidation of β-$Ni(OH)_2$ derived from the parent α-phase, but the cathodic peak corresponded to γ-phase ($K_{0.33}NiO_2 \cdot 0.67H_2O$) reduction. The interpretation of the results of further studies by MacArthur [9], using pre-cycled sintered plate electrodes containing mainly β-$Ni(OH)_2$, was that the main anodic peak at 0.5 V with respect to Hg/HgO/KOH was due to the formation of β-NiOOH but, again surprisingly, the larger and most cathodic peak at ~ 0.23 V was considered to be reduction of the γ-phase. MacArthur suggested that the γ-phase was produced at higher anodic potentials and a shoulder on the oxygen evolution branch at 0.57 V was assumed to be related to this process.

Recently Paszkiewicz and Walas [10] have reported voltammetric data for sintered plate electrodes. These workers considered the least cathodic reduction peaks (at ~ 0.4 V with respect to Hg/HgO/KOH) to be related to the reduction of unstable NiO_2 or the γ-phase, and the most cathodic peak (at ~ 0.3 V with respect to Hg/HgO/KOH) as the reduction of β-NiOOH. Such assignments are at variance with the observations by MacArthur [6, 9], Bode *et al.* [7, 8] and also with the reversible potential data for bulk nickel hydroxide/oxyhydroxide phases [2 - 5].

Sintered plate electrodes have an important advantage compared with thin film electrodes; the larger weights of active material present make it possible to perform supplementary chemical and X-ray diffraction analyses and so establish the phases present [5, 11]. Furthermore, by measuring the volumes of oxygen evolved during charging at slow sweep rates, it is possible to determine the oxidation states of the phases present in the electrode. The use of such supplementary techniques is central to the understanding developed in this study.

This paper will consider mainly the initial oxidation behaviour of ordered β-$Ni(OH)_2$ and cyclic oxidation/reduction behaviour within the β-phase system. Cyclic behaviour where the γ-phase is present will be the subject of a further publication.

2. Experimental

2.1. Linear sweep voltammetry and coulometry

The technique was similar, but refined, compared with that described previously [5]. The apparatus consisted of a potentiostat (Chemical Elec-

tronics, TR40/3A), linear sweep unit (L.S.U.I.), coulometer (constructed at BGTC) and three X–Y recorders. Voltammograms were plotted simultaneously using an instrument with a logarithmic amplifier in the Y-axis (Bryans 26000/A4) and also with a normal linear amplifier in the Y-axis (Bryans 21004). Coulograms were displayed on the third X–Y plotter (Minigor 510). Potentials and charge were also monitored using digital voltmeters (Bradley 173 B).

2.2. Potentiostatic charging

In some experiments oxidation of β-$Ni(OH)_2$ was carried out by applying a potentiostatic-step initiated by a wave-form generator (Hi-Tek PP-RI). The potential was stepped from 0 V to between 0.55 and 0.85 V.

2.3. E_r measurements

Measurements of quasi-reversible potentials, E_r, for the starting materials were made using the techniques described elsewhere [2].

Approximate E_r values were also determined at selected points in the voltammetric sweeps. Anodic decay transients were observed after interrupting the sweep at the anodic limits. Cathodic recovery transients were observed similarly after interrupting the sweep at the desired cathodic peaks. The E_r values were calculated from the decay and recovery E *vs.* t curves in the usual manner [2].

2.4. Cell

The triple-compartment glass cell used is depicted in Fig. 1. A 2 or 5 ml burette in the working compartment enabled the oxygen evolved from the working electrode to be measured. Corrections were made for atmospheric pressure, partial vapour pressure and hydrostatic pressure. The electrolyte (7M KOH) was pre-saturated with O_2 before the measurements. Voltammograms and coulograms were recorded within the range 0.8 - 0.05 V against the Hg/HgO/7M KOH reference electrode. All measurements were made at 22 ± 2 °C. The voltammograms shown are not corrected for ohmic drop.

2.5. Electrode materials

Sintered plate electrodes containing β-$Ni(OH)_2$ were used as described previously [5, 11]. The starting materials and oxidation products were characterised by X-ray diffraction [11]. The plates normally employed in the measurements contained ~ 0.09 g of $Ni(OH)_2$ in a sample size of 1 cm × 1 cm. The precise weights of active material were taken into account for the individual electrodes used for accurate measurements of oxidation states.

3. Results and discussion

3.1. First cycle anodic oxidation of β-$Ni(OH)_2$

Figures 2 and 3 show typical first cycle oxidation curves obtained in 7M KOH using combined linear sweep voltammetry and oxygen evolution

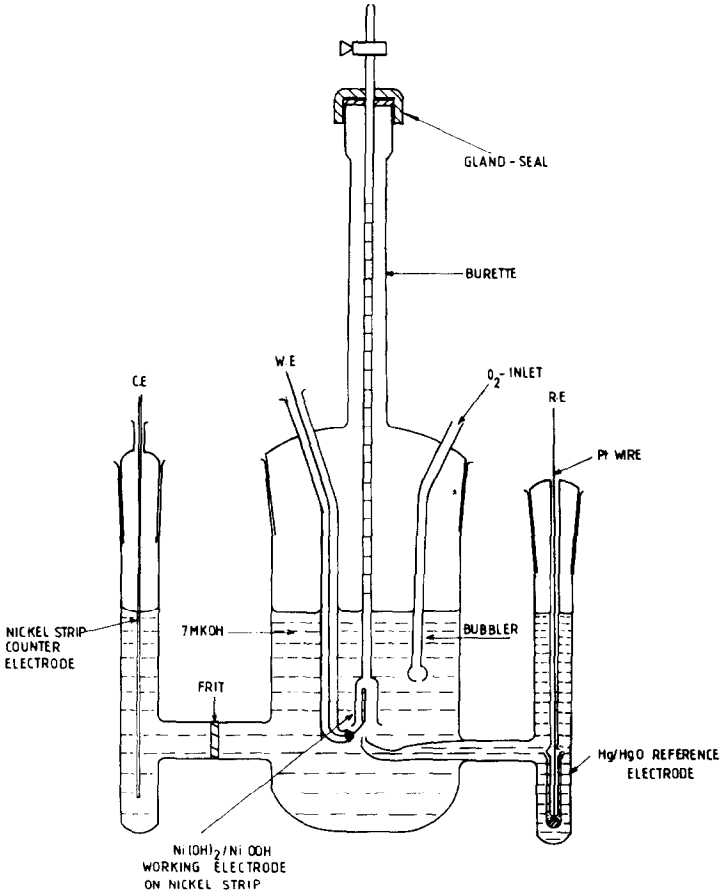

Fig. 1. Electrochemical cell.

measurements. These results were obtained for two samples of sintered plate electrodes designated A and B containing β-$Ni(OH)_2$ prepared by chemical precipitation between 3M $Ni(NO_3)_2$ and 7M KOH at 90 °C. Sample A was digested at 90 °C in 7M KOH for 0.5 h while sample B was digested for ~ 1.5 h. Sample A, giving rise to Fig. 2, was found by X-ray diffraction to be more disordered [5] than sample B, giving rise to Fig. 3. The difference in crystallinity is also reflected in the reversible potentials; sample A having an E_r of 0.414 V compared with 0.453 V with respect to Hg/HgO/7M KOH for sample B. It has been demonstrated previously [5] that ordered β-$Ni(OH)_2$ samples usually give rise to couples having higher E_r values.

A slow sweep rate of 0.005 V/min was required to give any indication of the shoulder near 0.6 V on the first anodic scan for the most ordered

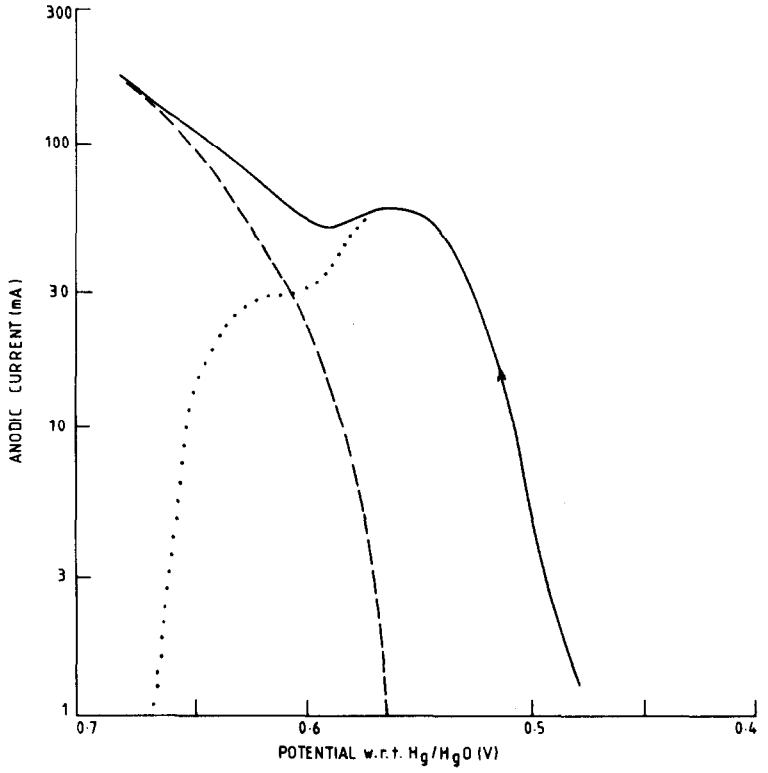

Fig. 2. First cycle voltammogram for anodic oxidation of β-$Ni(OH)_2$, sample A, in 7M KOH. Sweep rate 0.005 V/min. ——, Total current; - - - -, oxygen current; ·····, active material oxidation current.

sample B. At 0.01 V/min this feature was not clearly resolved (see also, later, Fig. 5).

The broken lines in Figs. 2 and 3 relate to the oxygen evolution current component calculated at frequent intervals during the measurements from the volumes of oxygen evolved. The dotted lines in Figs. 2 and 3 correspond to the active material oxidation current obtained by difference between the total current and the oxygen current. When this is taken into account, oxidation peaks can be clearly identified at ~ 0.56 V and ~ 0.61 V in Fig. 2 and at ~ 0.59 and ~ 0.66 V in Fig. 3. Figures 4 and 5 show the derived active material oxidation current curves at the two sweep rates of 0.005 and 0.01 V/min, respectively, together with peak deconvolutions where possible.

Areas under the oxidation peaks were evaluated by Simpson's method using a programme for the CBM 3032 (PET) computer. The areas in Fig. 5 corresponded to electron changes of ~ 0.9 *e* for the peak at 0.59 V and 0.6 *e* for the one at 0.66 V, *i.e.*, a total electron change of 1.5 *e*. Clearly, the first peak at ~ 0.59 V must be due to oxidation of β-$Ni(OH)_2$ to β-NiOOH (or

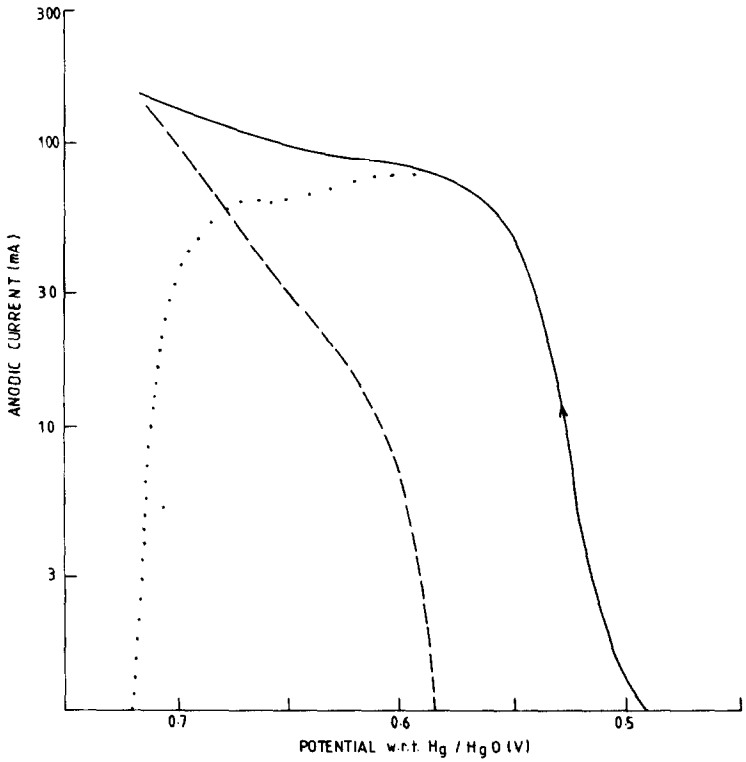

Fig. 3. First cycle voltammogram for oxidation of β-$Ni(OH)_2$, sample B, in 7M KOH. Sweep rate 0.005 V/min. ——, Total current; - - -, oxygen current; ·····, active material oxidation current.

phase V) whilst the second at 0.66 V corresponds to further oxidation of β-NiOOH to the γ-phase $K_{0.33}NiO_2 \cdot 0.67H_2O$ (or phase V_1).

From a comparison of Figs. 4 and 5, it is apparent that the oxidation peaks occur at less anodic potentials for the more disordered β-$Ni(OH)_2$, sample A. This is particularly evident for the most anodic peak at slow sweep rates. Thus, for the disordered β-$Ni(OH)_2$ some conversion of β-NiOOH to the γ-phase would always be expected at potentials more anodic than ~ 0.55 V. For the rest of this study the more ordered material B has been chosen.

Our observation for the formation of β-NiOOH from β-$Ni(OH)_2$ at relatively high anodic potentials differs from that generally accepted in the literature. MacArthur [9] ascribed the shoulder near 0.57 V on the oxygen evolution branch of the voltammogram for extensively cycled sintered plate electrodes to conversion of β-NiOOH to the γ-phase. Oxidation of β-$Ni(OH)_2$ to β-NiOOH is usually considered to take place at ~ 0.5 V (*cf.* MacArthur [9]), and is indeed the case with more disordered β-$Ni(OH)_2$ or materials produced on cycling, as will be discussed presently (Section 3.4.).

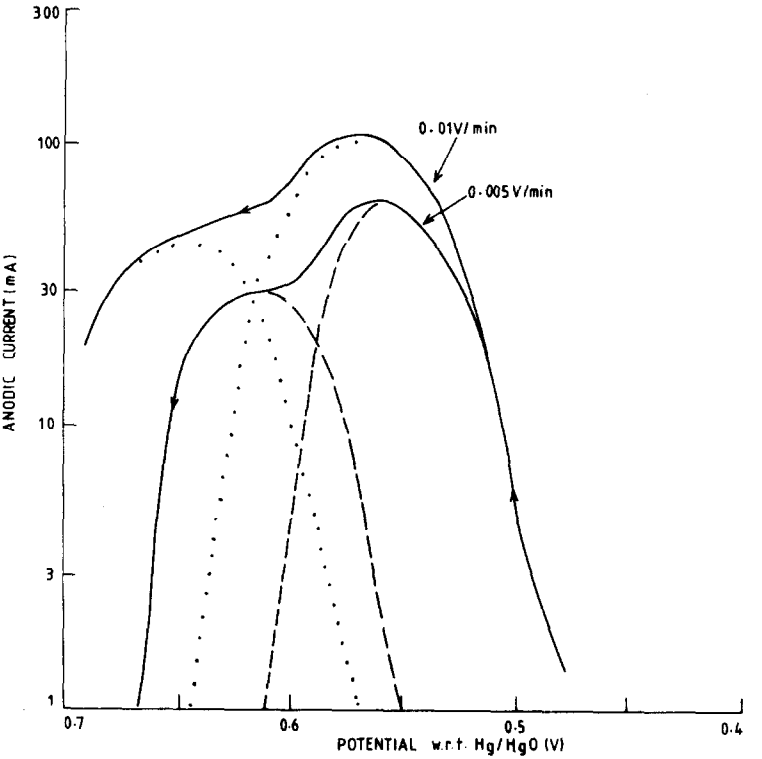

Fig. 4. Corrected voltammograms for first cycle oxidation of sample A with peak deconvolutions. - - - -, Sweep rate 0.005 V/min; ·····, sweep rate 0.010 V/min.

It is tempting to suggest that the differences in oxidation potential relate entirely to differences in lattice order of the parent β-$Ni(OH)_2$ or the U/V couple derived therefrom [2, 5]. Samples of chemically precipitated β-$Ni(OH)_2$ prepared in 1M KOH at room temperature can be shown [12] to have a highly disordered structure and a correspondingly low E_r value of 0.400 V with respect to Hg/HgO/1M KOH. These materials give rise to a well defined, single 0.9 e oxidation peak at ~ 0.46 V on the first oxidation cycle. Detailed ageing studies [5] on β-$Ni(OH)_2$, however, have revealed that shifts in oxidation potential of up to 100 mV can occur after ageing sintered plate electrodes in 7M KOH at 70 °C without significantly altering the E_r value.

The precise shape and position of the first oxidation wave for β-$Ni(OH)_2$ is clearly influenced by other important kinetic factors. The abnormal behaviour of β-$Ni(OH)_2$ after ageing in hot KOH is probably related to changes at the active material surface rendering the initial oxidation process difficult. Nickel hydroxide is a low conductivity p-type semiconductor which depends, for its proper functioning, on the development of a space-charge region in the outer-surface layer. Later injection of Ni^{3+} ions into the bulk then increases the active material conductivity. It is also possible that small changes in lattice order could strongly influence the ease of nucleation

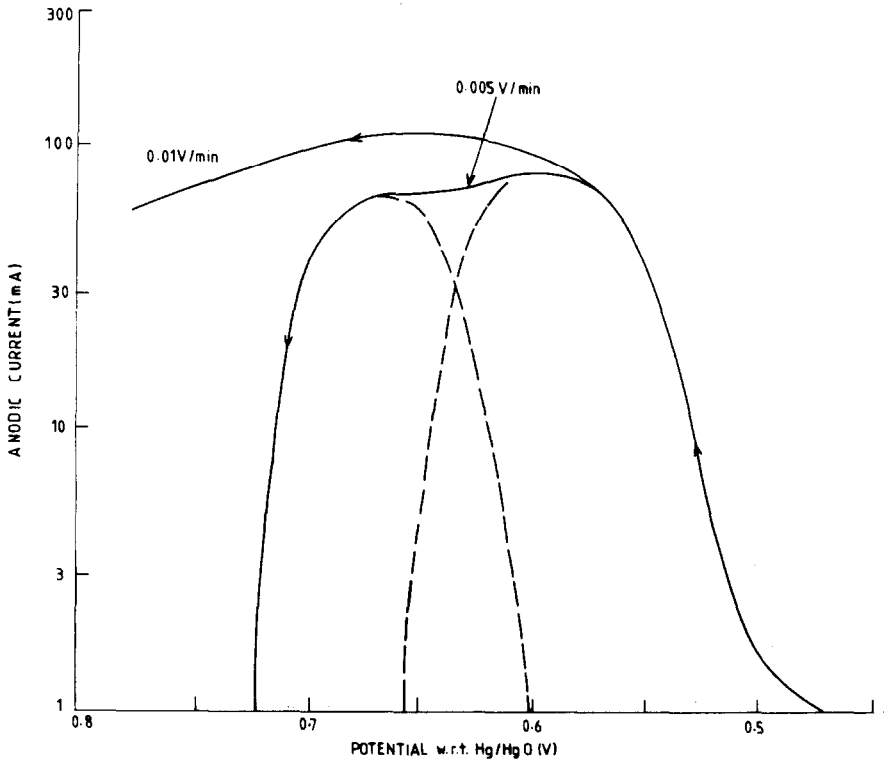

Fig. 5. Corrected voltammograms for first cycle oxidation of sample B with peak deconvolutions. - - - -, Sweep rate 0.005 V/min; ·····, sweep rate 0.010 V/min.

of the coexisting phases U and V from within the initially homogeneous Ni^{2+}/Ni^{3+} oxidised zone [2, 3]. Thus the development of an initial oxidised surface layer on the nickel hydroxide and subsequent nucleation restrictions could be accompanied by appreciable overpotentials in certain cases.

3.2. Oxidation of β-Ni(OH)$_2$ at constant potential

Sample B was oxidised potentiostatically at various potentials in the range 0.55 - 0.85 V with respect to Hg/HgO/7M KOH until a desired nickel oxidation state had been reached. This anodic treatment was then followed by a single cathodic linear potential scan at 0.01 V/min to ~ 0.15 V. The results obtained for a nickel oxidation state of 2.1 are depicted in Fig. 6(a) - (f). It can be seen that for oxidation potentials up to 0.6 V (Fig. 6(a) and (b)) a single cathodic peak is found at ~ 0.41 V. Higher anodic potentials (*e.g.*, 0.75 V) allow an additional reduction process to be found in the region 0.35 V and below (Fig. 6(f)).

Figure 7(a) - (e) shows data obtained by the above procedure except with the nickel oxidation state increased to 2.4. After oxidation at 0.55 V a broad cathodic peak can be found on reduction at ~ 0.34 V (Fig. 7(a)) with a slight shoulder at ~ 0.3 V. When the oxidation potential is increased to 0.6

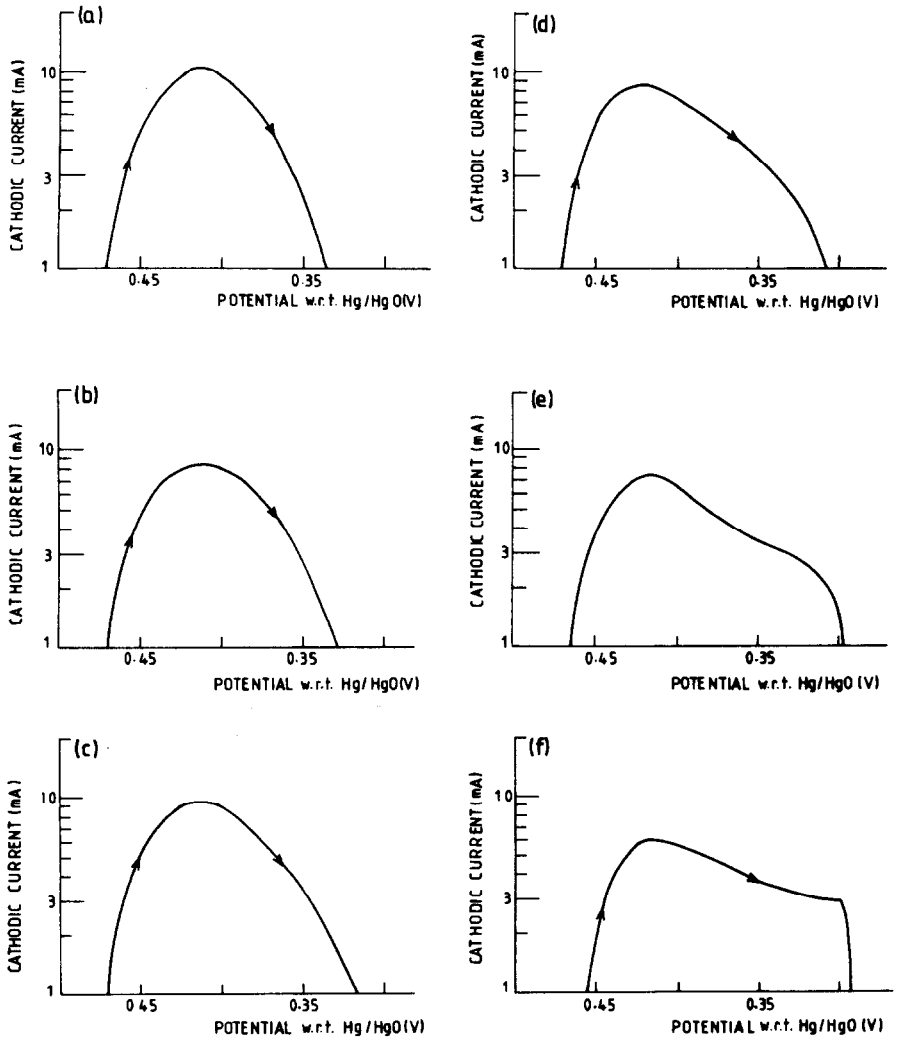

Fig. 6. Cathodic voltammograms after potentiostatic oxidation of β-$Ni(OH)_2$, sample B, in 7M KOH at various potentials to the same fixed oxidation state of 2.1. Oxidation potentials: (a) 0.55 V, (b) 0.60 V, (c) 0.65 V, (d) 0.70 V, (e) 0.75 V, (f) 0.85 V. Sweep rate 0.010 V/min.

V (Fig. 7(b)) this shoulder is better resolved and at oxidation potentials of 0.65 V and above (Fig. 7(c) - (e)) appears as a secondary peak at ~ 0.29 V. At the same time the broad maximum appears at a slightly less cathodic potential of ~ 0.39 (*cf.* 0.41 V in Fig. 6(a)).

From Fig. 5, previously discussed, it would be expected that if the oxidation potential does not exceed 0.6 V then the system should remain predominantly within the β-phase. This observation was confirmed by X-ray diffraction. Consequently, the cathodic reduction peaks at 0.39 V or 0.41 V

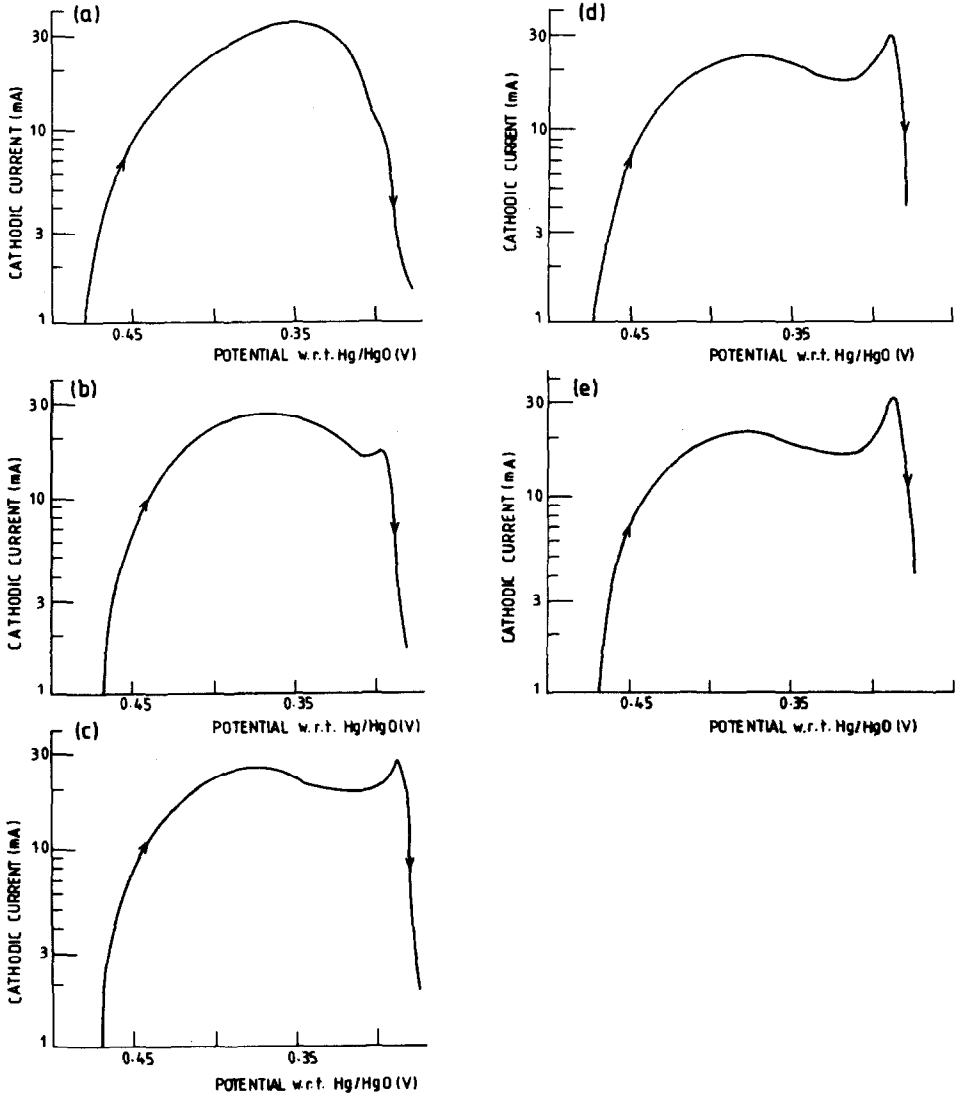

Fig. 7. As Fig. 6 with final oxidation state of 2.4.

and at 0.36 V must be related to reduction of Ni^{3+} species within the β-phase system, *i.e.*, phase V → phase U. When the oxidation potential exceeds 0.6 V, however, then γ-phase (V_1) formation is clearly possible, even if the total nickel oxidation state is as low as 2.1 - 2.4. Thus, the sharp peak which develops on the cathodic wave at ~ 0.29 V, where the oxidation potential exceeds 0.6 V as in Fig. 7(b) - (e), can be assigned to the reduction of phase V_1 → phase U_1 involving Ni^{4+} and Ni^{2+} species [2]. The phase U_1, relating to the α-$Ni(OH)_2$ structure, is unstable and may revert to phase U in the β-phase system with loss of inter-layer water. The more cathodic displacement of the

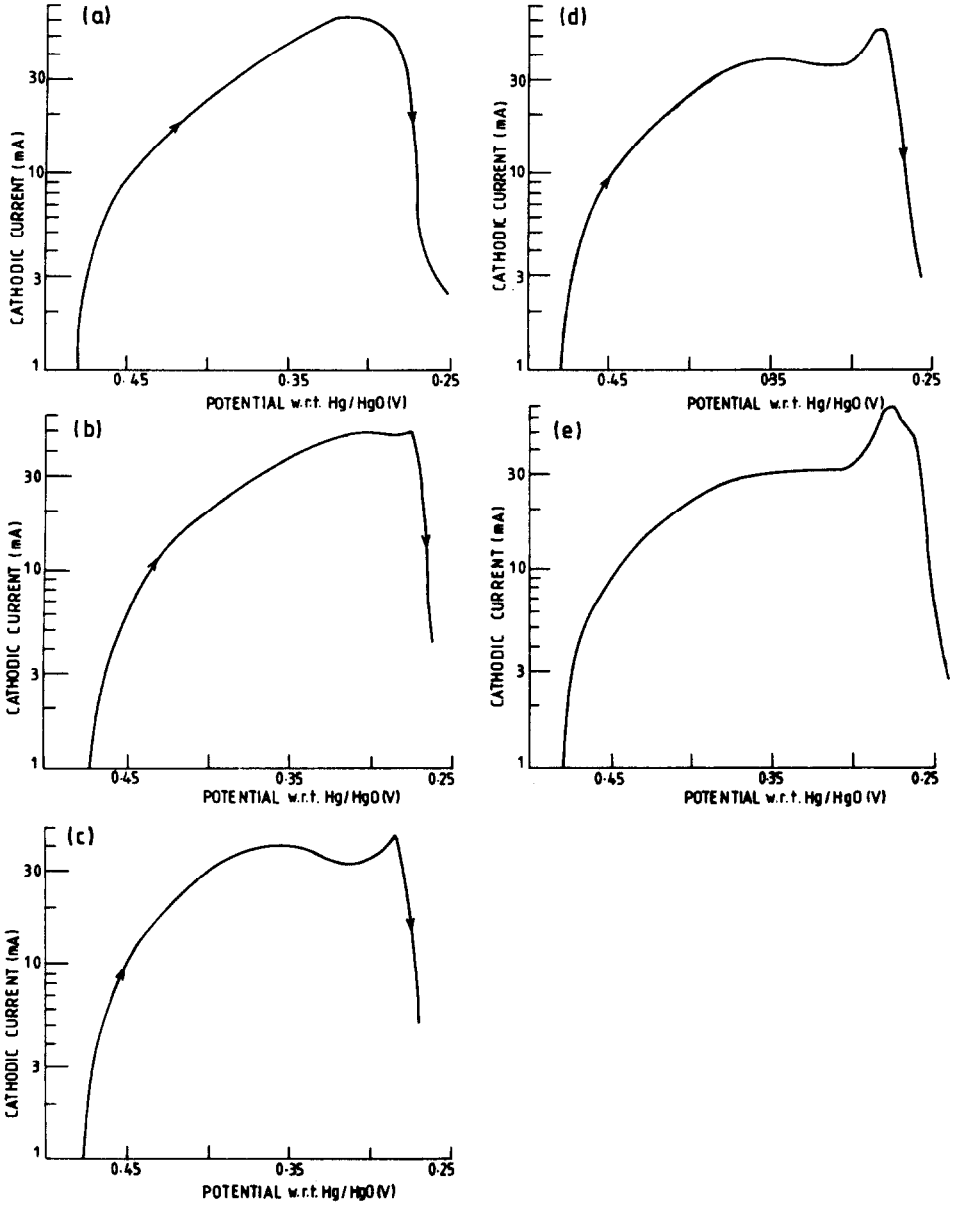

Fig. 8. As Fig. 6 with final oxidation state of 2.7.

γ-phase reduction potential is consistent with previously measured E_r values [2], and with the presence of γ-phase lines in the diffraction pattern.

Figure 8(a) - (e) shows data obtained at a nickel oxidation state of 2.7. Similar features can be observed to those in Fig. 7(a) - (e) except that the reduction peaks have shifted to slightly more cathodic values for a given

applied oxidation potential. Oxidation at 0.55 V (Fig. 8(a)) causes the subsequent broad reduction peak to appear at ~ 0.31 V. This process is still most likely to be due to reduction of phase V within the β-phase system, as will be discussed in Section 3.4. Higher oxidation potentials (0.65 V) show separation (Fig. 8(c)) of the corresponding reduction peaks at ~ 0.36 V and ~ 0.28 V in a similar way to those observed in Fig. 7(a) - (e). The sharp peak at ~ 0.28 V is likely to be due to reduction of phase V_1 to phase U_1 as before.

3.3. Cyclic voltammetry and coulometry

Tables 1 - 3 give complete coulometric data for sample B operating in 7M KOH. These measurements were obtained during cyclic voltammetry at 0.01 V/min to fixed anodic limits of 0.55, 0.6 and 0.65 V, respectively. Figures 9(a) - (c), 10(a) - (c) and 11(a) - (c) show the first three cycles relating

TABLE 1

Coulometric data obtained during cycling voltammetry at 0.01 V/min between potential limits of 0.55 and 0.05 V with respect to Hg/HgO/7M KOH for β-$Ni(OH)_2$, sample-B (a 1 *e* change equivalent to 89.9 coulombs)

Cycle no.	Charge input per cycle (C)	Charge due to O_2 (C)	Charge remaining after discharge (C)	Oxidation state	
				At end of charge	At end of discharge
1	15.6	0.0	6.2	2.175	2.070
2	26.1	0.3	5.9	2.360	2.133
3	32.2	0.2	4.4	2.493	1.180
4	43.3	0.6	4.1	2.660	2.219
5	50.9	0.8	4.6	2.783	2.262
6	63.5	1.7	5.7	2.957	2.307
7	73.0	2.3	7.7	3.102	2.368
8	83.9	3.7	10.2	3.270	2.441

TABLE 2

Coulometric data obtained during cycling voltammetry at 0.01 V/min between potential limits of 0.6 and 0.1 V with respect to Hg/HgO/7M KOH for β-$Ni(OH)_2$ sample-B (a 1 *e* change equivalent to 93.6 coulombs)

Cycle no.	Charge input per cycle (C)	Charge due to O_2 (C)	Charge remaining after discharge (C)	Oxidation state	
				At end of charge	At end of discharge
1	51.6	2.0	16.8	2.551	2.158
2	66.5	2.4	11.7	2.843	2.257
3	74.1	2.4	7.5	3.024	2.312
4	87.1	3.3	14.5	3.207	2.432
5	98.1	10.0	20.2	3.372	2.541
6	97.1	10.1	14.1	3.459	2.573

TABLE 3

Coulometric data obtained during cyclic voltammetry at 0.01 V/min between potential limits of 0.65 and 0.15 V with respect to Hg/HgO/7M KOH for β-$Ni(OH)_2$ sample - B (a 1 *e* change ≡ 93.6 coulombs)

Cycle no.	Charge input per cycle (C)	Charge due to O_2 (C)	Charge remaining after discharge (C)	Oxidation state	
				At end of charge	At end of discharge
1	117.7	11.2	52.6	3.138	2.442
2	111.2	20.8	38.0	3.408	2.626
3	115.4	35.5	37.8	3.480	2.651

to these data. In some cases, in order to increase the oxidation state above 2.66, it was necessary to hold the sweep at the anodic limit for a short time.

It should be noted that the oxidation state reached on anodic treatment includes contributions on both the forward anodic scan to the anodic limit and the reverse scan to zero current. It is inadmissible to assume [10] that the current on the reverse scan derives solely from oxygen evolution, although, of course, the quantity of oxygen evolved from the electrode increases with increasing oxidation state of the nickel.

True oxidation states were calculated from the coulometer and evolved oxygen measurements as before, which takes into account the fact that the cathodic, as well as the anodic processes were not 100% efficient, as found previously [11].

The charge remaining after the cathodic sweep (see Tables 1 - 3) was added to the charge supplied on successive anodic cycles. It should also be noted that, because of the non-uniform charging characteristics [2] of sintered plate electrodes, even at oxidation states below the measured least oxidised co-existing phase limit [4] of 2.25, both co-existing phases are present in addition to a large proportion of unoxidised β-$Ni(OH)_2$.

In Fig. 9(a) where the anodic limit is fixed at 0.55 V and the nickel oxidation state at 2.18, a single cathodic peak is again found at ~ 0.40 V (*cf.* Fig. 6(a)), for the reduction of phase V to phase U. Increasing the oxidation state to 2.36 (Fig. 9(b)) leads to the emergence of a second cathodic peak at ~ 0.32 V in addition to the one at ~ 0.40 V. At an oxidation state of 2.5 (Fig. 9(c)) an asymmetric peak maximum appears at ~ 0.31 V.

If the anodic potential limit or the holding time are increased then the shift in cathodic peak maximum to more cathodic potentials takes place even more rapidly, as illustrated by Fig. 10(a) - (c). In this case the anodic limit has been increased to 0.6 V and the cathodic maxima shift to potentials of 0.3, 0.26, and 0.25 V at nickel oxidation states of 2.55, 2.84, and 3.02, respectively. At oxidation states of 2.84 some γ-phase (V_1) is also likely to be present, as suggested by the marked cathodic peak displacement to ~ 0.25 V. Again a significant reduction process can be observed in the 0.4 V region at all oxidation states, up to 3.02.

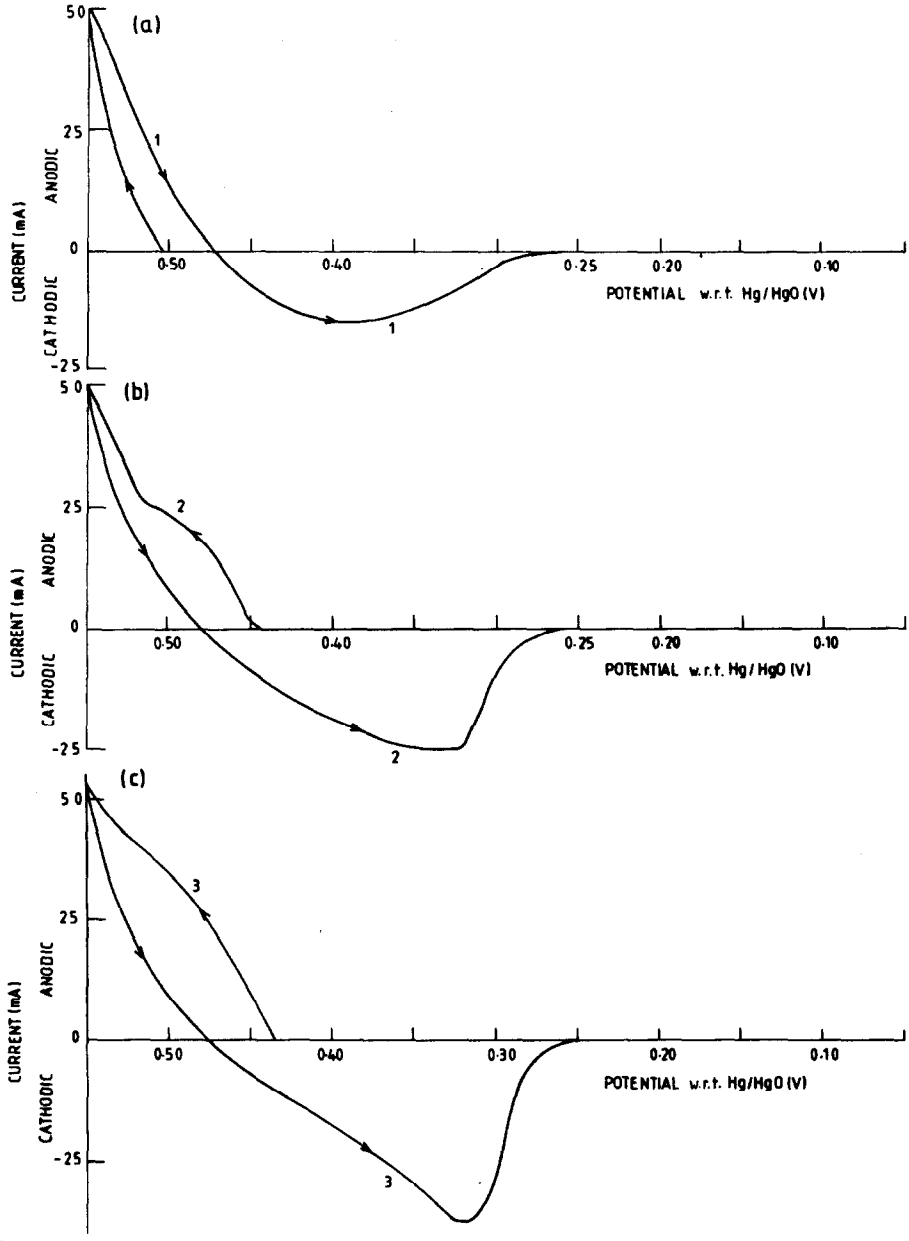

Fig. 9. Consecutive cyclic voltammograms for β-$Ni(OH)_2$, sample B, in 7M KOH at 0.01 V/min between 0.05 and 0.55 V. Nickel oxidation states after anodic scan: (a) 2.18, (b) 2.36, (c) 2.49.

Figure 11(a) - (c) shows the result of increasing the anodic limit to 0.65 V. The corresponding cathodic peak appears at 0.25 V at an oxidation state of 3.14, and at 0.21 V at an oxidation state of 3.48. At total oxidation states

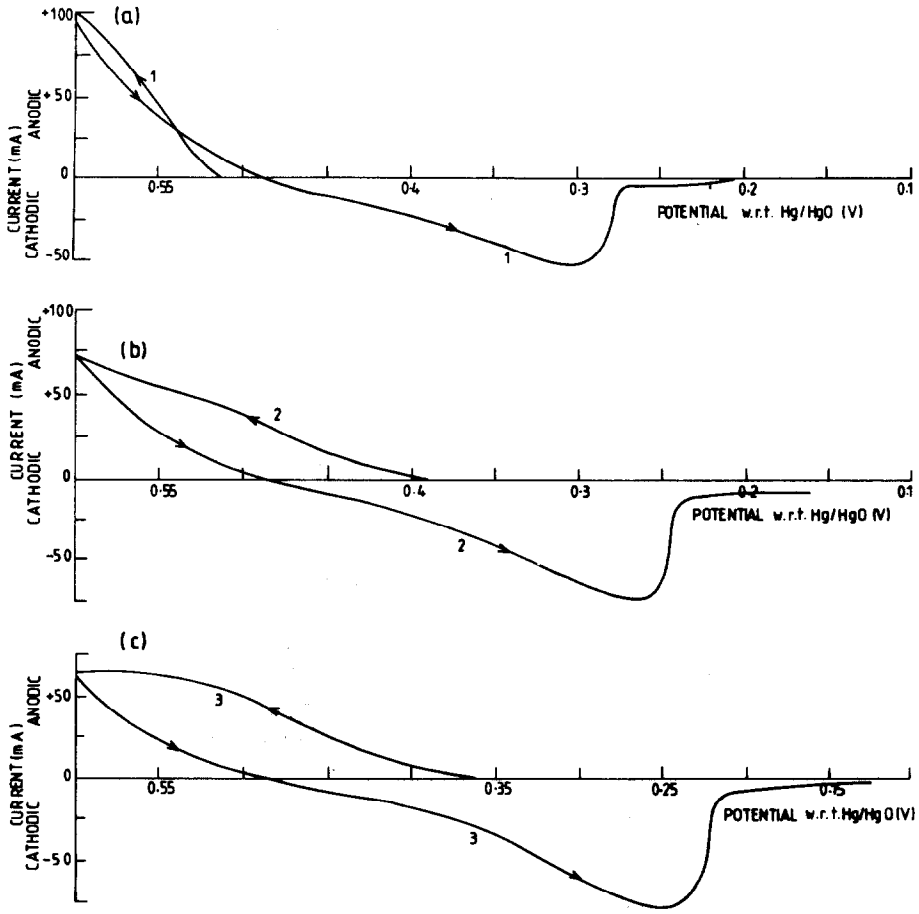

Fig. 10. Consecutive cyclic voltammograms for β-$Ni(OH)_2$, sample B, in 7M KOH at 0.01 V/min between 0.1 and 0.6 V. Nickel oxidation states after anodic scan: (a) 2.55, (b) 2.84, (c) 3.02.

above 3.0 a considerable proportion of the γ-phase ($K_{0.33}NiO_2 \cdot 0.67H_2O$) must be present. Figure 11(c) shows the additional feature of two well defined oxidation peaks near 0.5 and 0.57 V; the voltammogram resembling that previously reported by MacArthur [9].

It should be noted that the shifts in cathodic potentials cannot be accounted for in terms of ohmic drop alone. A measured resistance of ~ 0.15 Ω between the working and reference electrodes would cause changes of, at the most, 10 mV. In practice the peak-shifts are an order of magnitude higher.

Micka *et al.* [13] have suggested that multiple cathodic peaks on discharge can be caused by ohmic drop between different parts of the electrode structure, particularly in the case of polytetrafluoroethylene (PTFE)-bonded nickel hydroxide electrodes. The effect was simulated using two sintered

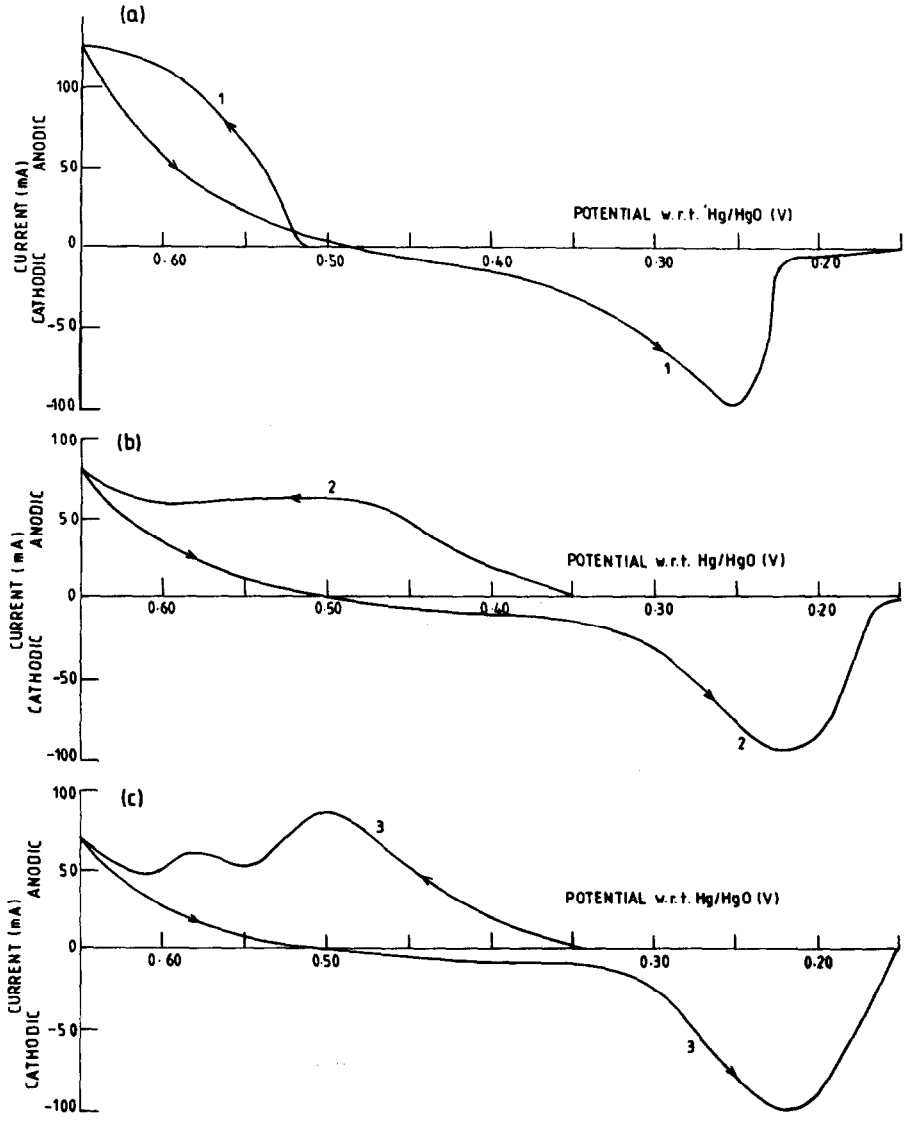

Fig. 11. Consecutive cyclic voltammograms for β-$Ni(OH)_2$, sample B, in 7M KOH at 0.01 V/min between 0.65 and 0.15 V. Nickel oxidation states after anodic scan: (a) 3.14, (b) 3.41, (c) 3.48.

plate electrodes connected in parallel with a resistance (10 Ω) in series with one electrode. The observation was used primarily to explain the cause of the secondary discharge steps, as discussed also by Barnard *et al.* [3]. Internal ohmic effects within the sintered electrode were considered to be negligible.

It should be noted that porous sintered plate electrodes would be expected to show greater reaction distribution and ohmic effects internally

compared with a thin film electrode. This would be manifest in terms of broader and more asymmetric peaks. Nevertheless, multiple anodic and cathodic peaks can still be observed for thin film electrodes as will be discussed in a separate communication.

It will become apparent in the next section that the shifts or multiplicity of voltammetric peaks cannot arise entirely from ohmic or porous electrode effects. A considerable degree of shifting can be related directly to shifts in equilibrium potential which are independent of current and, therefore, of ohmic effects. In the explanation offered by Micka *et al.* [13] the reversible potential would be assumed to be essentially constant.

3.4. Cause of peak shifting

As demonstrated previously, in Figs. 9(a) - (c), 10(a) - (c) and 11(a) - (c), cyclic oxidation/reduction appears to lead to a progressive "activation" of the β-phase lattice, perhaps as a consequence of increasing disorder developing in both U and V phases. This effect is accompanied by a progressive shift in the reduction potential for the process V $\rightarrow$ U from $\sim$ 0.40 to 0.32 V.

Shifts in potential can be related directly to a change in the reversible potential of the electrode. Figure 12 shows plots of quasi-reversible potentials, E_r, as a function of the initial oxidation state for species present near the peak maxima in Figs. 9(a) - (c) and 10(a) - (c). It can be seen that E_r falls by about 70 mV from a nickel oxidation state of 2.1 to about 3.0. At oxidation states above 3.0, where the γ-phase (V_1) is largely determining the potential, the E_r value for the V_1/U_1-couple remains relatively constant at 0.34 V. The results shown in Fig. 12 preclude the cathodic shifts in voltammetric peaks being caused entirely by ohmic or by other dynamic effects during the sweep. The changes in E_r must be related to changes in free energy between different pairs of coexisting U and V phases within the β-phase layer lattice system, or to the presence of U_1/V_1 couples where the γ-phase has been produced.

The relatively wide spectrum of E_r values for the β-phase system is most likely to be responsible for the broad characteristics of the reduction peaks which can span more than 100 mV. By comparison, the γ-phase (V_1) reduction peaks are considerably narrower (Figs. 7(a) - (e) and 8(a) - (e)). It has been shown previously [11] that the galvanostatic reduction of β-NiOOH (phase V) is accompanied by more sloping discharge curves compared with the γ-phase.

The broad reduction peaks for the β-phase are best regarded as envelopes embracing several U/V couples, each involving different free energies of reaction, rather than to single processes. From the e.m.f. data alone it is not possible to relate any change in disorder which may have been induced specifically to the oxidised or reduced phase.

It must be emphasised that the previous charging history critically influences the fall in E_r value with the nickel oxidation state. By application of suitable experimental techniques the decline found in Fig. 12 can be circumvented.

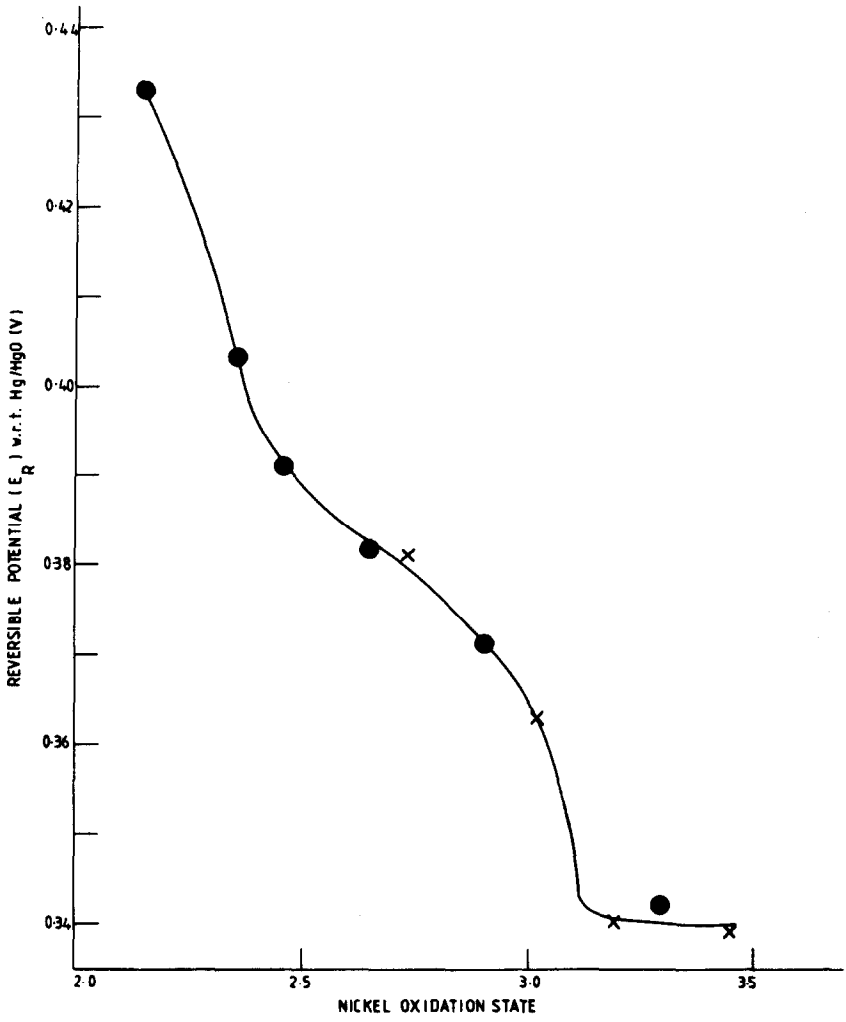

Fig. 12. Variation of reversible potential, E_r, for species present at the cathodic peak maxima as a function of nickel oxidation state for different anodic limits. ●, anodic limit, 0.55 V; ×, anodic limit, 0.60 V.

It has been demonstrated previously [2] that, by allowing only small increments of charge to pass through the active material, it is possible to restrain the U/V couples to largely the same free energy band. For example, sample B was found to give an E_r value of 0.453 V with respect to Hg/HgO/7M KOH which remained constant over the oxidation range from 2.25 to 2.7, unlike the downward sloping central section of Fig. 12. If this material was charged in a single stage to an oxidation state of 2.67, discharged and

allowed to remain in the discharged state for 24 h before remeasuring the potential, however, the E_r value was found to fall to 0.427 V. This couple was termed "activated" to distinguish it from the parent "deactivated" couple. In both cases the slight dependence of E_r on alkali and water activity ($\sim$ 0.1 mole KOH/2*e* transfer) led one to conclude that the β-phase lattice was retained, as confirmed by X-ray diffraction methods [11]. The lowering in reversible potential was attributed to disordering within the lattice as a consequence of the oxidation/reduction process [2, 3].

Further studies [5], in which a range of β-$Ni(OH)_2$ samples were prepared having various levels of lattice disorder (as inferred by X-ray diffraction), indicated that disorder in the starting material was a common feature for β-phase couples having the lower reversible potentials.

The potentiostatic oxidation experiments (Figs. 6(a) - (f), 7(a) - (c) and 8(a) - (c)) indicated that the application of a high anodic potential alone need not necessarily cause a fall in potential for the β-phase couple when the alternative formation of the γ-phase (V_1) also takes place. In Fig. 7(a) - (e) a reduction peak at $\sim$ 0.4 V for the process V $\rightarrow$ U still remains in addition to the sharp peak at $\sim$ 0.27 V due to the process $V_1 \rightarrow U_1$. If the anodic potential is restricted (*e.g.*, 0.55 V) to limit γ-phase (V_1) formation, however, then a broad cathodic peak appears centred at $\sim$ 0.34 V for an oxidation state of 2.4 (Fig. 7(a)). The fall in reduction potential again appears to be related to the fall in E_r found in Fig. 12 and suggests that the free energy of formation of the oxidised phase V is influenced by the coulombic intake of the β-phase lattice.

Cyclic oxidation/reduction processes have the secondary important consequence of allowing oxidation to take place at progressively less anodic potentials. For example, in Section 3.1. (Figs. 3 and 5) it was shown, starting with "ordered" β-$Ni(OH)_2$, that oxidation to β-NiOOH (phase V) reached a maximum near 0.59 V. Voltammetric cycling allows the main oxidation process to shift to less anodic potentials ($\sim$ 0.50 V) as in Figs. 9(a) - (c), 10 (a) - (c) and 11(a) - (c).

Concurrent studies have shown [12] that the oxidation process at $\sim$ 0.46 V may involve either oxidation of U $\rightarrow$ V within the β-phase or $U_1 \rightarrow V_1$ within the α/γ-phase system. These so called [2, 5] "activated" β- and "deactivated" α/γ-phase couples may be distinguished by the difference in dependence of E_r with alkali and water activity. Although α-phase materials containing interlayer water may be absent during the initial oxidation of "ordered" β-$Ni(OH)_2$, the least oxidised coexisting phase U_1 related to the α-structure can be produced indirectly on subsequent cycles *via* discharge of the γ-phase (V_1) produced by oxidation of phase V at higher anodic potentials. It may be recalled [4] that both phases U and U_1 have the same nickel oxidation state (*viz.*, 2.25). The intermediate phase U_1 may also be derived directly from nickel hydroxide samples showing initially either α- or β-type diffraction patterns, and this may lead to additional confusion [12].

Describing the oxidation/reduction processes in terms of respective pairs of coexisting phases [2 -5] helps to avoid such structural ambiguities.

Whether or not a material showing a β-phase diffraction pattern will oxidise directly to the γ-phase (V_1) in a single, two-electron-step process (analogous to true α-phase starting materials) is thought to depend on the relative ease with which water and KOH may be readmitted to the interlayer structure in the initial stages of oxidation. Formation of phase V_1 from a β-phase starting material normally occurs *via* a phase V intermediate involving two separate single electron transfer stages, as demonstrated earlier.

Although the oxidation peak at ~ 0.58 V observed in Fig. 11(c) could be ascribed to oxidation of β-$Ni(OH)_2$ to β-NiOOH (or phase U → phase V) as on the first cycle, it is likely that γ-phase formation is also taking place in this region (*cf.* MacArthur [9]) from species involving smaller free energies of reaction than in the initial case.

Where voltammetric scans have been allowed to reach a high anodic limit (> 0.6 V), oxidation/reduction peaks may involve the overlap of several U/V and U_1/V_1 couples, even though only a β-phase starting material was employed. This factor makes unambiguous peak assignments difficult.

A more detailed discussion of the voltammetric behaviour for mixed U/V and U_1/V_1 systems will be given in a later paper. This investigation emphasises the importance of full characterisation of active material before attempting more detailed kinetic studies.

Acknowledgements

The authors thank the Directors of Berec Group Limited for permission to publish this work and Dr F. L. Tye for helpful discussions.

References

1 G. W. D. Briggs, *Electrochemistry*, Vol. 4, Specialist Periodical Reports, The Chemical Society, London, 1974, p. 33.
2 R. Barnard, C. F. Randell and F. L. Tye, *J. Appl. Electrochem.*, *10* (1980) 109.
3 R. Barnard, C. F. Randell and F. L. Tye, *J. Appl. Electrochem.*, *10* (1980) 127.
4 R. Barnard, C. F. Randell and F. L. Tye, *J. Electroanal. Chem.*, *119* (1981) 17.
5 R. Barnard, C. F. Randell and F. L. Tye, in J. Thompson (ed.), *Power Sources 8*, Academic Press, London, 1981, p. 401.
6 D. M. MacArthur, *J. Electrochem. Soc.*, *117* (1970) 422.
7 H. Bode, K. Dehmelt and J. Witte, *Electrochim. Acta*, *11* (1966) 1076.
8 H. Bode, K. Dehmelt and J. Witte, *Z. Anorg. Allg. Chem.*, *366* (1969) 1.
9 D. M. MacArthur, in D. H. Collins (ed.), *Power Sources 3*, Oriel Press, Newcastle upon Tyne, 1971, p. 91.
10 M. Paszkiewicz and I. Walas, *Electrochim. Acta*, *24* (1979) 629.
11 R. Barnard, G. T. Crickmore, J. A. Lee and F. L. Tye, *J. Appl. Electrochem.*, *10* (1980) 61.
12 R. Barnard, C. F. Randell and F. L. Tye, in R. G. Gunther (ed.), *Proceedings of the Symposium on the Nickel Electrode, Vol. 82-4*, Electrochem. Soc. Inc., 1982, p. 69.
13 B. Klapste, J. Mrha, K. Micka, J. Jindra and V. Marecek, *J. Power Sources*, *4* (1979) 349.